Electronic Supplementary Material (ESI) for Journal of Materials Chemistry B.

Silica Nanovehicles Endow Arsenic Trioxide with Effective Treatment of Cancer Cells and Solid Tumors

*Zhenghuan Zhao, Hui Zhang, Xiaoqin Chi, Hui Li, Zhenyu Yin, Dengtong Huang, Xiaomin Wang, and Jinhao Gao**

Supplementary Information

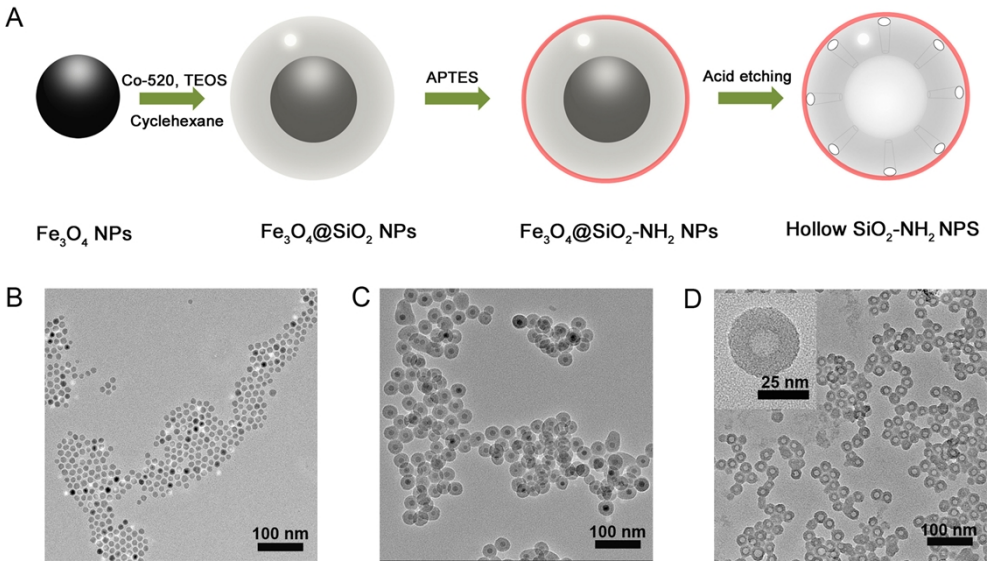

Fig. S1. Synthesis of hollow SiO_2-NH_2 (HSNs) nanoparticles. (A) Schematic cartoon shows the synthesis of HSNs. TEM images of (B) Fe_3O_4, (C) Fe_3O_4@SiO_2-NH_2, and (D) HSNs nanoparticles (inset, high-magnification TEM image), respectively.

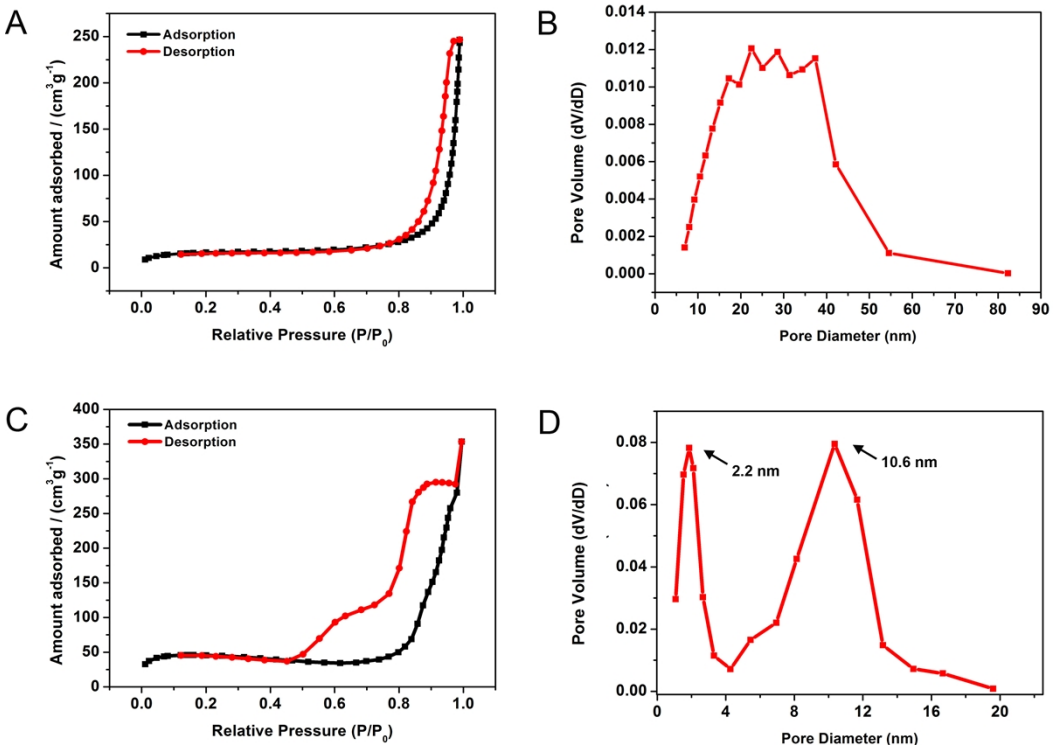

Fig. S2. Characterization of HSNs. (A, C) The nitrogen adsorption-desorption isotherms and (B, D) the corresponding pore size distribution of the Fe_3O_4@SiO_2 and HSNs nanoparticles derived from desorption isotherm measurement and BJH methods, respectively.

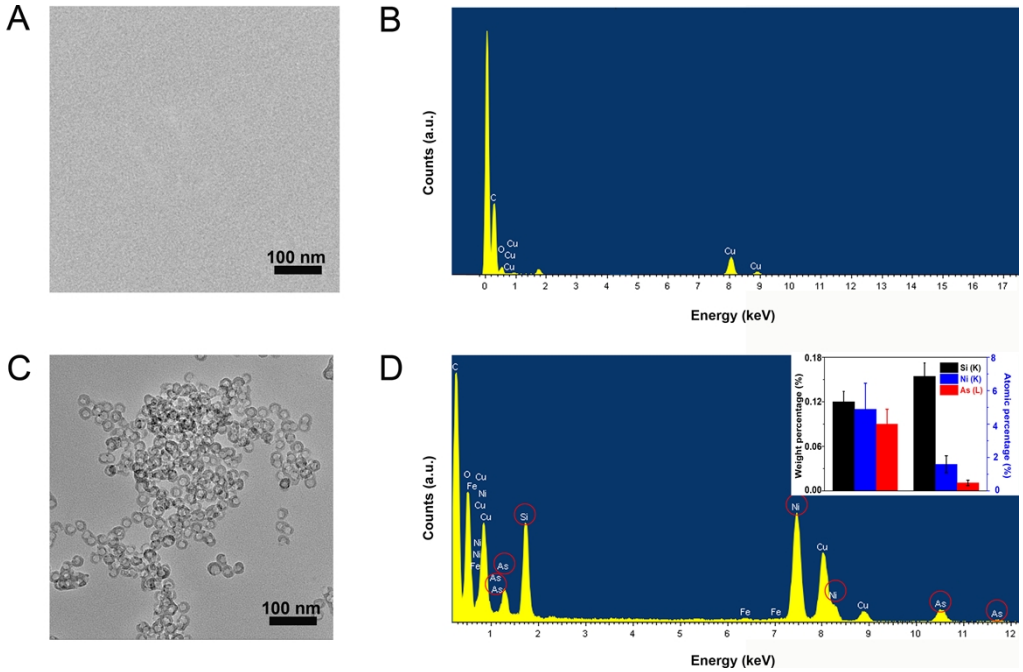

Fig. S3. Analysis of the Ni,As@SiO_2 nanoparticles by energy dispersive X-ray spectroscopy (EDS). The TEM images of (A) the blank region and (C) the region of Ni,As@SiO_2 nanoparticles in the same copper mesh sample. The EDS analysis corresponding to (B) blank region and (D) accumulative Ni,As@SiO_2 nanoparticles region, insert is the quantified EDS profile of Ni,As@SiO_2, revealing the successful accumulation of Ni and As in the HSNs.

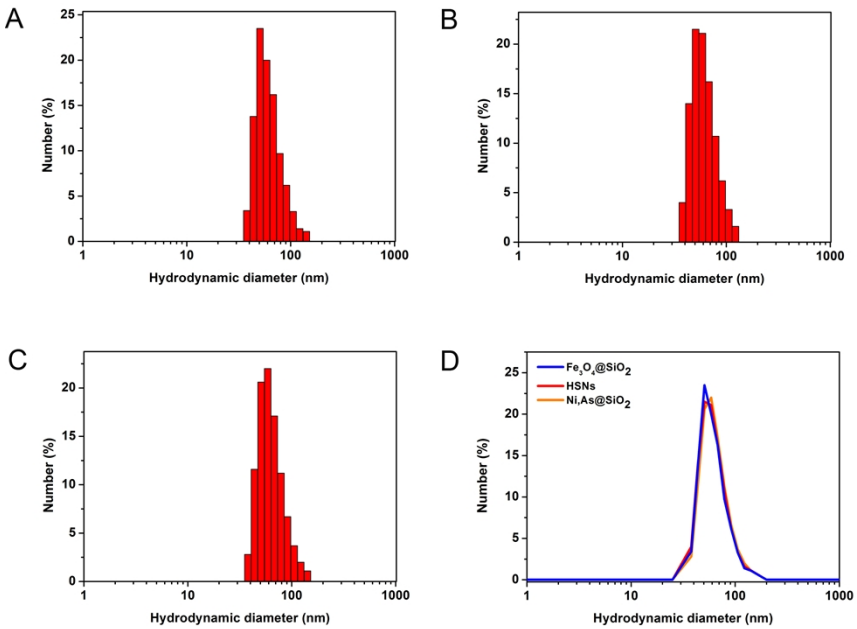

Fig. S4. DLS analysis of the water-dispersible nanoparticles. DLS profiles of (A) Fe_3O_4@SiO_2, (B) HSNs, and (C) Ni,As@SiO_2 nanoparticles, respectively. (D) The merged DLS profiles of all three samples, indicating that these three samples have the similar size distribution.

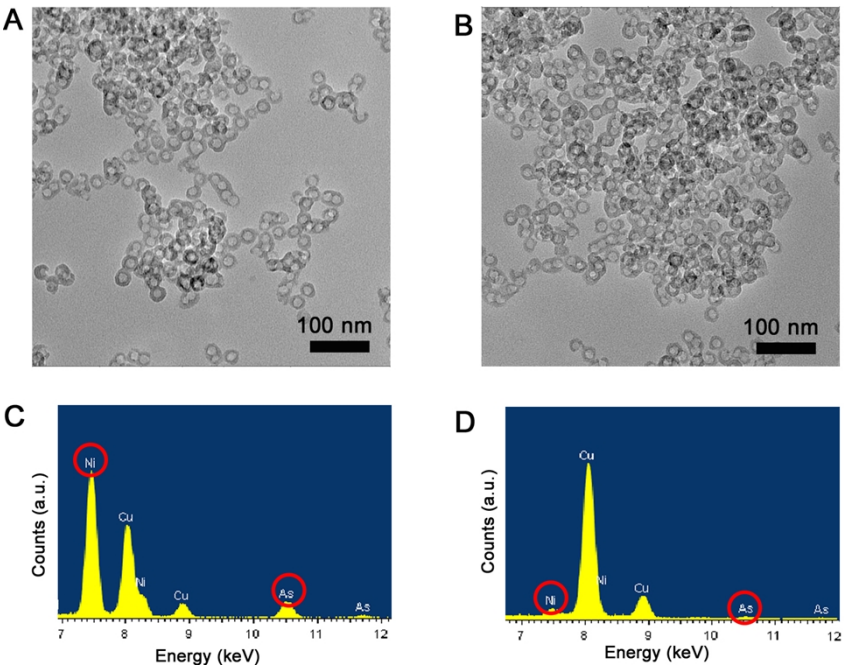

Fig. S5. TEM and energy dispersive X-ray spectroscopy (EDS) analysis of the Ni,As@SiO_2 nanoparticles. The TEM images of Ni,As@SiO_2 nanoparticles (A) before and (B) after drug releasing process. The EDS analysis corresponding to the region of Ni,As@SiO_2 nanoparticles (C) before and (D) after drug releasing process.

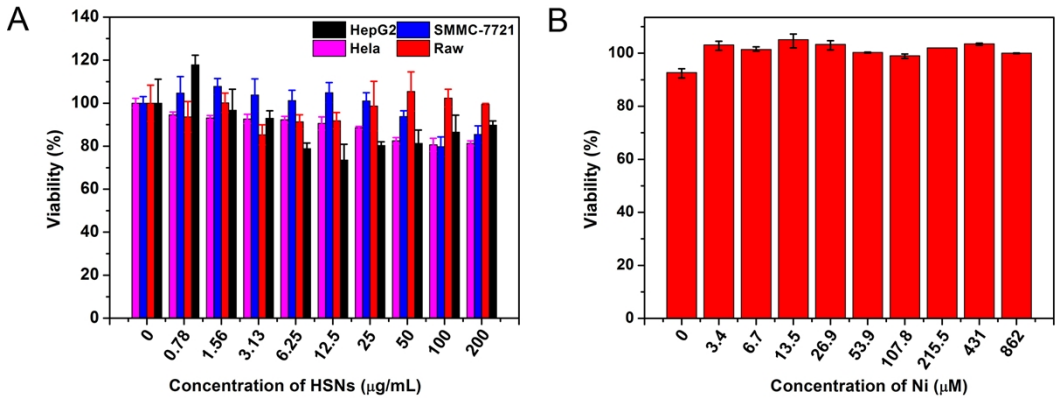

Fig. S6. *In vitro* cytotoxicity of HSNs and Ni ions. (A) The MTT assay of HeLa, RAW 264.4, HepG2, and SMMC-7721 cells incubated with multi-concentration of HSNs for 48 h, respectively (n = 5/group). (B) The MTT assay of HeLa cells incubated with various concentration of Ni for 48 h (n = 5/group).

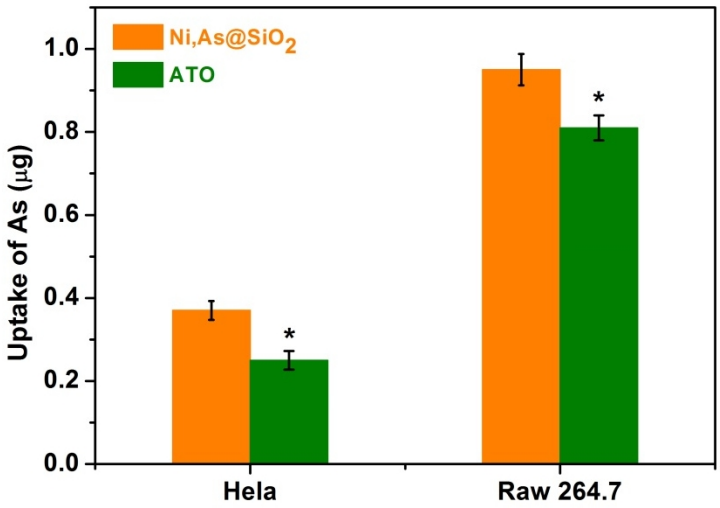

Fig. S7. The uptake amount of As in HeLa and RAW 264.7 cells after treated with ATO and Ni,As@SiO_2 for 4 h, respectively (n = 3/group). The error bars represent standard deviation of three independent experiments (*$p < 0.05$).

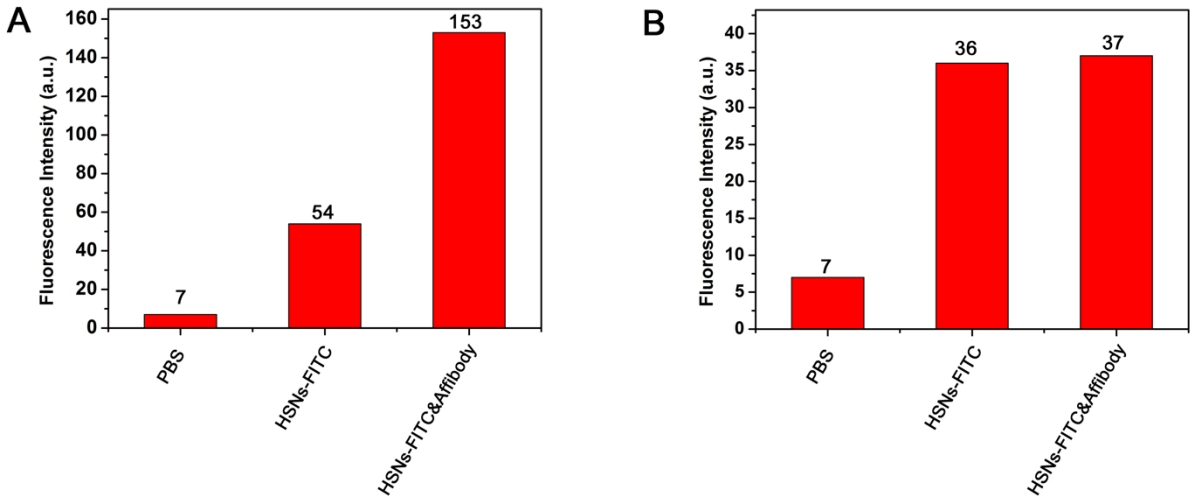

Fig. S8. Quantitative analysis of mean fluorescence intensity of (A) SMMC-7721 cells and (B) MCF-7 after incubation with HSNs-FITC and HSNs-FITC&Affibody with the same concentration of FITC for 24 h, respectively.

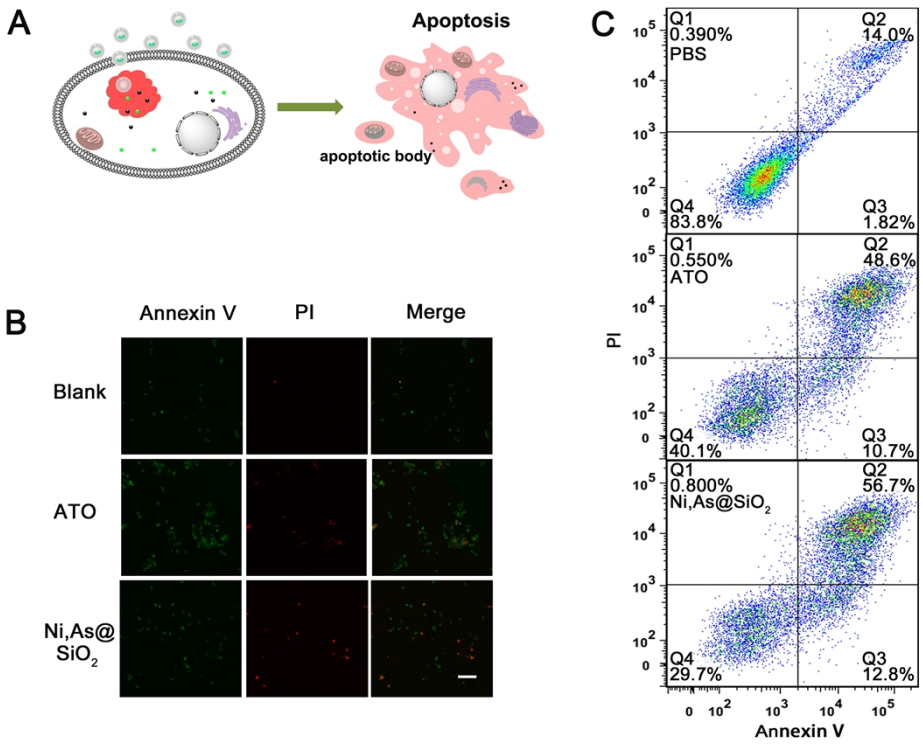

Fig. S9. The cytotoxic mechanism of Ni,As@SiO_2 nanomedicine. (A) Cartoon schematic shows the mechanism of Ni,As@SiO_2 to kill the cancer cells by apoptosis. (B) Fluorescent images and (C) quantitative flow cytometric analysis of SMMC-7721 cells after treatment with PBS, ATO, and Ni,As@SiO_2 for 24 h, respectively. Cells were stained with propidium iodide (PI) and Annexin-V for recognizing the phosphatidylserine presented on apoptosis cells at room temperature. Scale bar, 100 μm for all images.

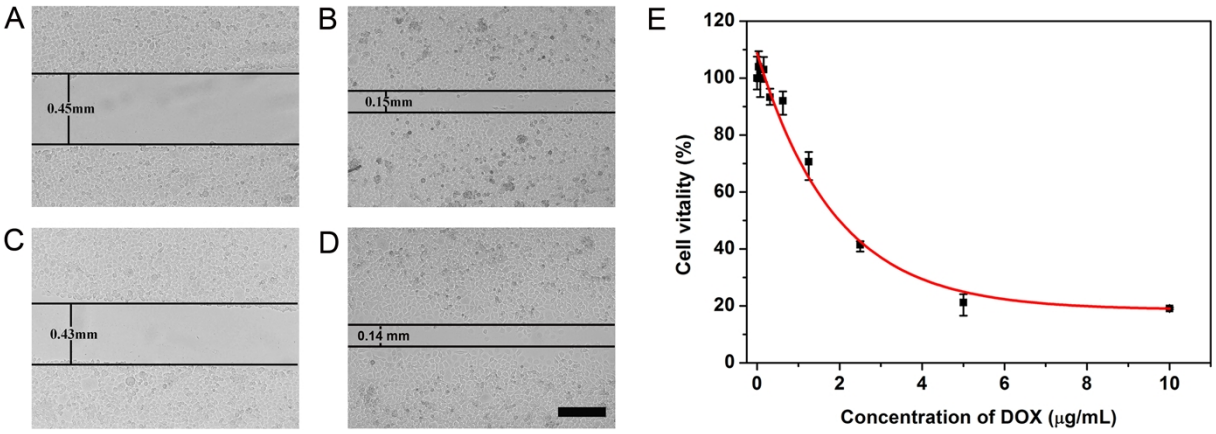

Fig. S10. Cell migration assay of SMMC-7721 cells. (A, C) The representative created gap on a layer of SMMC-7721 cells in 12-well plate. The gap after incubation with (B) PBS and (D) DOX (2 μg/mL, the IC_{50} concentration) for 24 h, respectively. Scale bar, 200 μm for all images. (E) The MTT assay curve of SMMC-7721 cells treated with DOX for 24 h, indicating the IC_{50} value for DOX to SMMC-7721 is about 2 μg/mL.

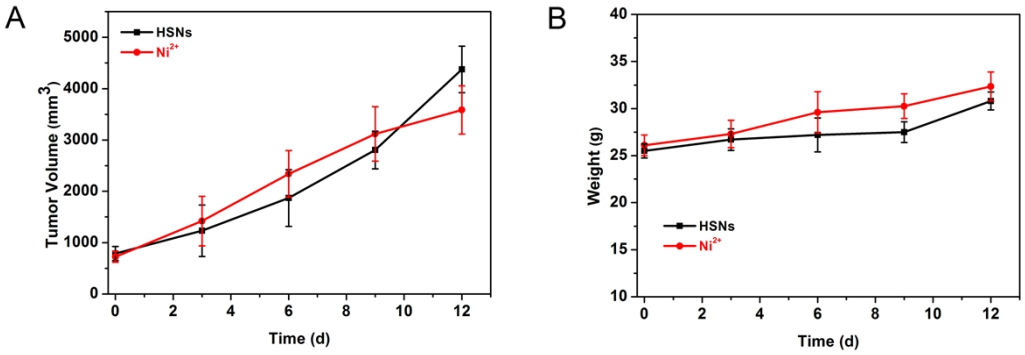

Fig. S11. *In vivo* study on the tumor model mice. (A) Tumor growth curves after intravenous injection of HSNs and Ni^{2+}. The arrows indicated the treatment time. (B) The body weight change curves of the mice during the treatment of HSNs and Ni^{2+}.

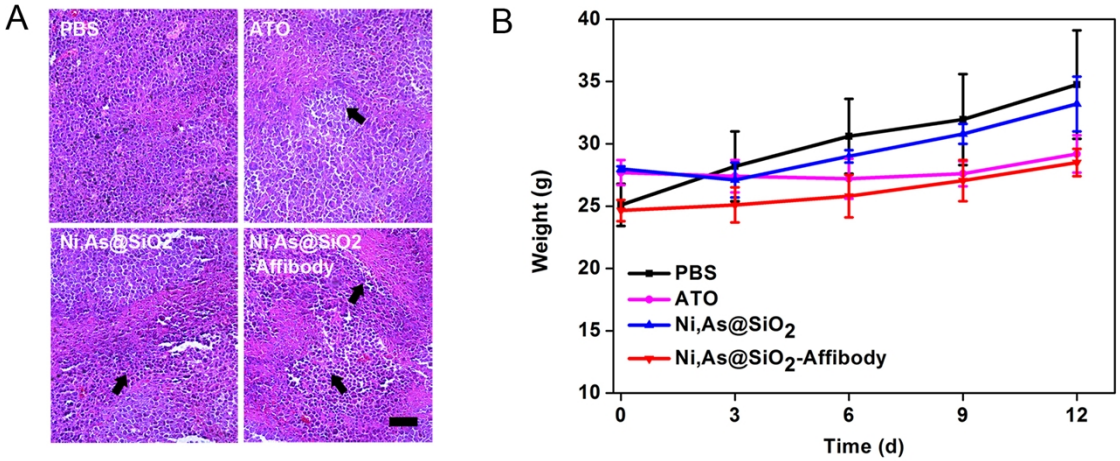

Fig. S12. *In vivo* study on the tumor model mice. (A) Histology images of the tumors collected from mice treated with PBS, ATO, Ni,As@SiO_2, and Ni,As@SiO_2-Affibody at the end of treatment. The black arrows indicated the typical necrotic cells in tumors. Scar bar: 100 μm for all images. (B) The body weight change curves of the mice during the treatment.

Table S1. The migration distance and ratio of SMMC-7721 after treated with the PBS, ATO, Ni,As@SiO_2, and Ni,As@SiO_2-Affibody with a dose of 13.3 μM, respectively (*n* =3).

	Migration distance (mm)	Migration ratio (%)
PBS	0.27 ± 0.020	100 ± 7.51
ATO	0.16 ± 0.007	59.4 ± 2.67
Ni,As@SiO_2	0.14 ± 0.017	50.9 ± 6.31
Ni,As@SiO_2-Affibody	0.12 ± 0.006	44.7 ± 2.36